

Soil and Sediment Contamination: An International Journal

ISSN: (Print) (Online) Journal homepage: www.tandfonline.com/journals/bssc20

Impact of Crude Oil Contamination and Low-Temperature Thermal Desorption on Soil Properties and Remediation Efficacy

Olubunmi Oluwadare Owoyemi, Lekan Olatayo Afolagboye, Megan Welman-Purchase & Damilola Tope Ogundele

To cite this article: Olubunmi Oluwadare Owoyemi, Lekan Olatayo Afolagboye, Megan Welman-Purchase & Damilola Tope Ogundele (07 Feb 2025): Impact of Crude Oil Contamination and Low-Temperature Thermal Desorption on Soil Properties and Remediation Efficacy, Soil and Sediment Contamination: An International Journal, DOI: 10.1080/15320383.2025.2461555

To link to this article: https://doi.org/10.1080/15320383.2025.2461555

Published online: 07 Feb 2025.

Submit your article to this journal

View related articles

View Crossmark data

Full Terms & Conditions of access and use can be found at
https://www.tandfonline.com/action/journalInformation?journalCode=bssc20

SOIL AND SEDIMENT CONTAMINATION: AN INTERNATIONAL JOURNAL
https://doi.org/10.1080/15320383.2025.2461555

Taylor & Francis
Taylor & Francis Group

Check for updates

Impact of Crude Oil Contamination and Low-Temperature Thermal Desorption on Soil Properties and Remediation Efficacy

Olubunmi Oluwadare Owoyemi[a], Lekan Olatayo Afolagboye[b], Megan Welman-Purchase[c], and Damilola Tope Ogundele[d]

[a]Department of Geology, Kwara State University, Ilorin, Nigeria; [b]Department of Geology, Ekiti State University, Ado-Ekiti, Nigeria; [c]Department of Geology, University of The Free State, Bloemfontein, South Africa; [d]Department of Chemistry, Kwara State University, Ilorin, Nigeria

ABSTRACT

Crude oil contamination significantly alters soil properties, posing environmental risks and challenges for sustainable development. This study investigates the potential of low-temperature thermal desorption (LTTD) at 110°C as an environmentally friendly remediation technique for crude oil-contaminated soils. Soil samples contaminated with crude oil from Nigeria's Niger Delta were analyzed for changes in Atterberg limits, specific gravity, linear shrinkage, sodium percentage (PS), and total dissolved solids (TDS). After LTTD treatment at 110°C for 30 minutes, the soils were assessed using gas chromatography, Fourier transform infrared spectrometry, X-ray diffraction, and scanning electron microscopy to evaluate microstructural and mineralogical changes. Contamination increased plasticity, shrinkage, and dispersivity, while reducing specific gravity. LTTD successfully removed up to 96% of hydrocarbons, but also caused a 15% weight change and minor alterations in hydrocarbon functional groups. Scanning electron microscopy revealed particle agglomeration after remediation, which may help counter the increased dispersivity caused by contamination. X-ray diffraction showed no significant mineralogical changes in the remediated soils. LTTD at 110°C proves effective in reducing hydrocarbons and mitigating crude oil-induced soil degradation, contributing to sustainable environmental management.

KEYWORDS

Environmental remediation; soil pollution; thermal remediation; erosion susceptibility

1. Introduction

Growing industrialization and urbanization have placed significant demands on the environment, leading to degradation and climate change (Kumar, Kumar, and Singh 2020, Nasir, Canh, and Lan Le 2021). Soil, a critical component of the environment, interacts dynamically with the atmosphere and water bodies (Wei et al. 2021). Efficient soil management, including contemporary treatments for contamination and erosion, is essential for achieving several United Nations Sustainable Development Goals, such as good health, zero hunger, and clean water and sanitation (Rodrigo-Comino et al. 2020). Furthermore, sustainable soil management is linked to food and water security, energy security, ecosystem

CONTACT Lekan Olatayo Afolagboye lekan.afolagboye@eksu.edu.ng; afotayour@hotmail.co.uk Department of Geology, Ekiti State University, Ado-Ekiti, P.M.B. 5363, Nigeria

© 2025 Taylor & Francis Group, LLC

services, biodiversity protection, and climate change mitigation (McBratney, Field, and Koch 2014).

Crude oil contamination remains one of the most severe global environmental challenges (Bashir et al. 2020; Buzmakov, Egorova, and Gatina 2019). Oil spills can occur during production, transportation, or storage, and may also result from natural seepage, sabotage, vandalism, or theft (Ukhurebor et al. 2021; Wizor and Wali 2020; Yeeles and Akporiaye 2016). While crude oil production has improved global living standards, it has also posed significant risks to aquatic and terrestrial ecosystems, causing land use disruption, alterations to the physical and chemical properties of soil and water, socio-economic challenges, and geotechnical problems (Bonatesta et al. 2022; Ghasemzadeh, Ostovar, and Karimi 2023; Magris and Giarrizzo 2020; Ostovar et al. 2021).

The global demand for oil continues to rise, increasing the frequency and scale of environmental pollution through oil spills (Kang et al. 2020). Nigeria, a leading oil producer, is among the top five countries most severely affected by petroleum-related environmental damage (Albert, Amaratunga, and Haigh 2018; Kadafa 2012). Data from the Nigerian Oil Spill Detection and Response Agency (NOSDRA) indicate that in 2022 alone, approximately 45,193.125 barrels of oil, equivalent to about 226 tanker trucks, were spilled into the Nigerian environment – a volume comparable to one-sixth of the Exxon Valdez oil spill in 1989 (260,000 barrels). Such spills have profound physical, ecological, and chemical impacts on the environment, contributing to widespread degradation and toxicity (Ndimele et al. 2018).

While extensive research has examined the ecological impacts of crude oil spills (Buzmakov, Egorova, and Gatina 2019), the effects on the geotechnical properties of soils have been less frequently reported, particularly in the context of tropical residual soils (Ostovar et al. 2021). High soil dispersivity, which has been linked to foundation failures, erosion, and subsidence, poses significant geotechnical risks (Hoseinimighani and Szendefy 2022; Savaş 2016; Vakili, Ghasemi et al. 2018; Vakili, Selamat et al. 2018). Dispersive soils, characterized by high levels of exchangeable sodium ions and susceptibility to erosion, present substantial challenges to infrastructure stability (Bell and Maud 1994; Umesh, Dinesh, and Sivapullaiah 2011; Yuan et al. 2021). Although research indicates that certain contaminants can increase soil dispersibility and erodibility (Chuchkalov, Fadeev, and Alekseev 2020; Portelinha et al. 2021), the specific effects of crude oil contamination on the dispersibility and erodibility of soils remain largely unexplored. Understanding how contaminants alter the physical and engineering properties of soils is crucial for effective soil management. Construction on contaminated soils requires an understanding of how contaminants have modified the soil's natural properties, often necessitating special engineering precautions rather than remediation alone. For example, changes in shear strength affect bearing capacity, while alterations in soil permeability influence consolidation rates and drainage properties.

Various remediation techniques have been employed to address crude oil contamination in soils, including physical, thermal, chemical, and biological methods (Ahmad 2020; Kang et al. 2020). Among these, thermal treatment is widely used due to its high removal efficiency, low cost, and relatively short treatment time (Liu et al. 2019; Merino and Bucalá 2007). Thermal treatment methods include thermal desorption and incineration, with incineration temperatures ranging from 730°C to 1200°C (Asghar et al. 2016) and thermal desorption occurring at either low (100–350°C) or high temperatures (350–600°C)

(Falciglia, Giustra, and Vagliasindi 2011). Due to its lower environmental impact and energy consumption, thermal desorption is preferred over incineration (Lim, Lau, and Poh 2016). Achieving effective remediation of crude oil-contaminated soils at lower temperatures is a more sustainable environmental management strategy.

This study investigates the influence of crude oil contamination on the properties of lateritic soils and assesses the effectiveness of LTTD as a remediation method at a drying temperature of 110°C.

2. Materials and methods

Four soil samples were collected from freshly exposed road cut materials at different locations along a major highway in southwestern Nigeria, as shown in Figure 1. To ensure uniformity in grain size, the samples were sieved through a No. 40 sieve to obtain particles finer than 425 µm. Grain size was considered a critical factor due to its impact on the efficiency of thermal desorption during the remediation of oil-contaminated soils (Falciglia, Giustra, and Vagliasindi 2011; Liu et al. 2019; Zhao et al. 2019)

Each soil sample, weighing 1 kg, was spiked with 150 mL (145 g) of crude oil sourced from the Nigerian Niger Delta, resulting in a contamination level of 145 g/kg or 150 mL/kg. The contaminated samples are shown in Figure 2. A portion of each contaminated sample (10 g) was subjected to a lab-scale remediation test through oven drying at 110°C for 30 minutes, which will henceforth be referred to as "remediation" in this article. After cooling at room temperature, the weight changes were recorded.

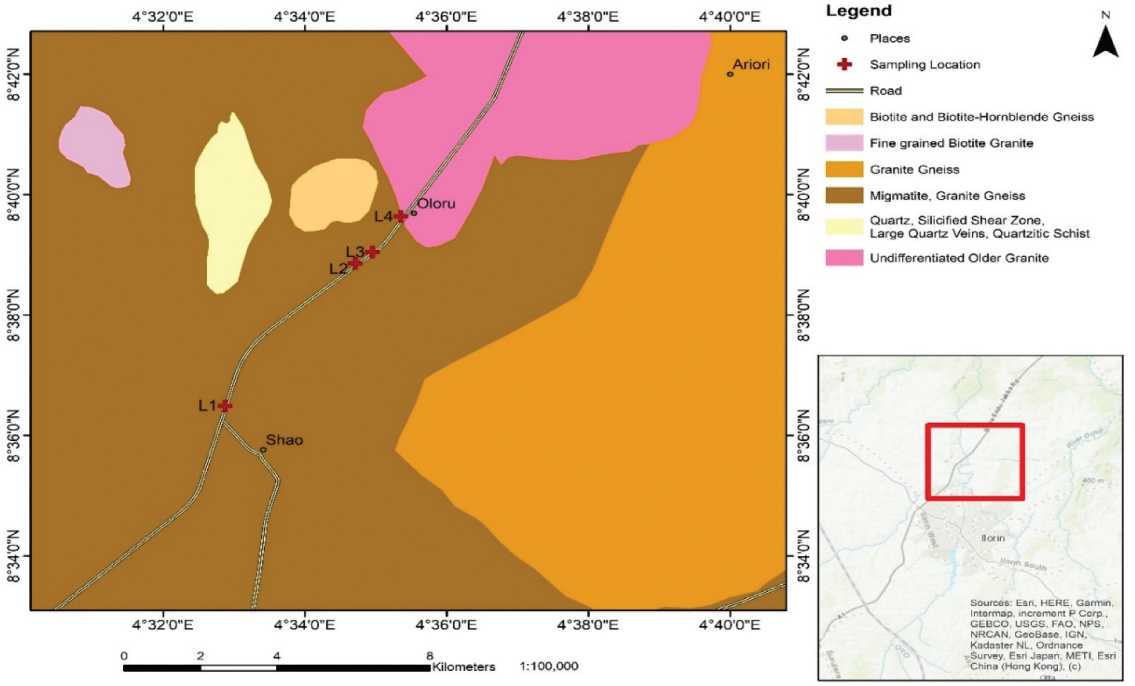


Figure 1. Geologic map showing sampling locations.

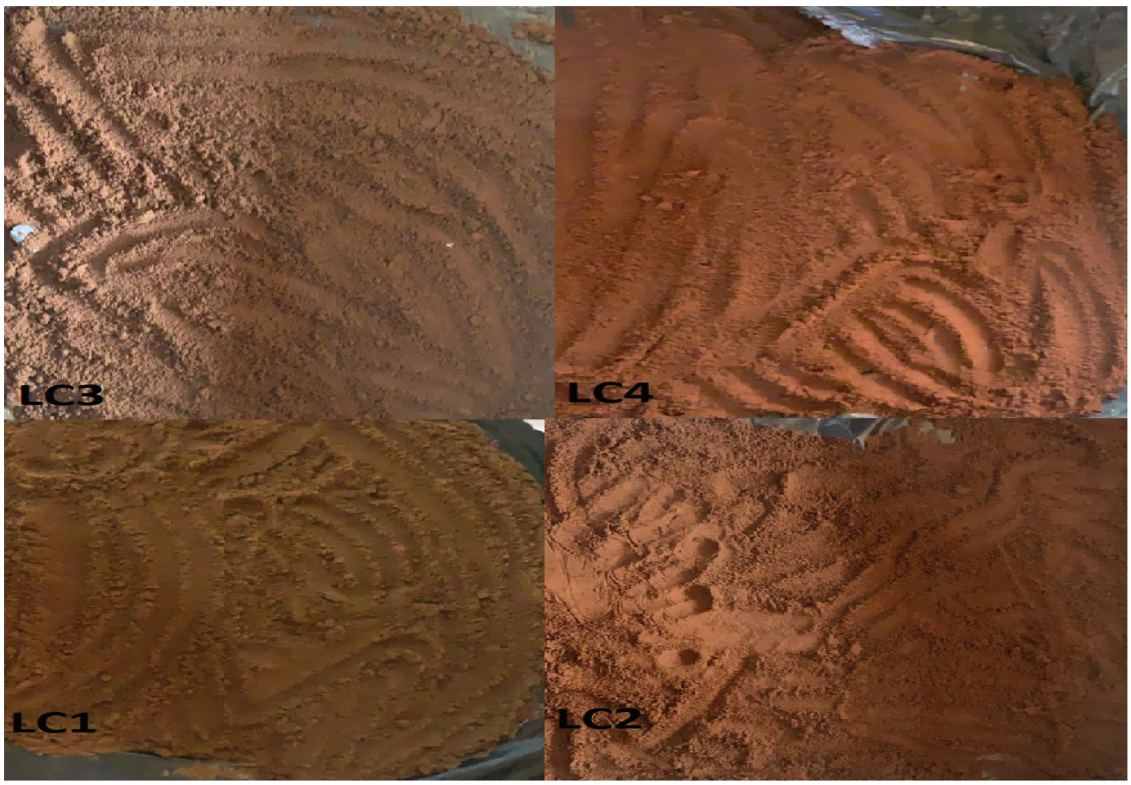


Figure 2. Contaminated soil samples.

The mineralogical composition of both the natural and remediated soil samples was analyzed using X-Ray Diffractometry (XRD) with a Malvern Panalytical Empyrean XRD, employing a copper tube at 40 mA and 45 mV, and measuring from 3.5° to 70° 2θ. The chemical composition was determined using X-Ray Fluorescence (XRF) with a 4 kW Rigaku Primus IV, equipped with a rhodium tube. Scanning Electron Microscopy (SEM) was performed on both natural and remediated samples to observe structural changes induced by contamination and remediation, using a Jeol JSM6610 with a tungsten filament, equipped with an Ultradry JED-2300 EDS.

Gas Chromatography Mass Spectrometry (GC-MS) was conducted on contaminated and remediated samples following a modified United States Environmental Protection Agency (EPA) extraction method (Method 8270C). The Total Petroleum Hydrocarbons (TPH) of the untreated and treated soil samples were determined. Hydrocarbons with the highest concentrations were identified and reported in this study based on the GC-MS library available for the analysis. While TPH encompasses a wide range of hydrocarbon compounds, this work specifically highlights those with the highest relative abundances in the samples. Each sample (5 g) was mixed with 5 g of anhydrous sodium sulfate and homogenized. The mixture was transferred to pre-cleaned extraction tubes, and 40 mL of dichloromethane was added. After standing for 30 minutes, the tubes were shaken vigorously for 30 minutes. The solvent layers were filtered using filter papers, and the procedure was repeated with 25 mL of dichloromethane. The extracts were combined, concentrated on a rotary evaporator, exchanged with 10 mL of n-hexane, and reconcentrated to 1 mL for cleanup. The cleaned extracts were analyzed for hydrocarbon content using a GC-MS

equipped with an Elite-5 MS (5% diphenyl/95% dimethylpolysiloxane) fused capillary column.

The removal efficiency (RE) was calculated using Equation 1:

$$RE(\%) = \frac{C_O - C}{C_O} * 100 \tag{1}$$

Where Co is the initial contaminant concentration in soil (mg/kg), and C is the residual concentration after thermal treatment.

Fourier Transform Infrared (FT-IR) spectroscopy was employed to analyze the chemical bonds in the contaminated and remediated samples using the potassium bromide pellet procedure. A mixture of 5 mg of soil and 1 g of potassium bromide was pressed at 34.5 MPa – 69 MPa and analyzed using an FT-IR Nicolet IS5 Thermoscientific machine. Each sample was scanned eight times. To assess the dispersivity potential of the soils, a chemical digestion method using Aqua Regia was performed. Each soil sample (1 g) was digested with 9 mL of concentrated nitric acid (HNO_3) and 3 mL of concentrated hydrochloric acid (HCl) in a digestion flask. After heating to expel brown nitrous fumes, the sample was cooled and filtered into a 50 mL standard flask. The filtrate was analyzed for Na^+, Ca^{2+}, Mg^{2+}, and K^+ using Atomic Absorption Spectroscopy (AAS). The ion concentrations (mg/L) were converted to milliequivalents per liter using Equation 2:

$$Milliequivalent = \frac{mg/l \times Valency\ of\ ion}{Molar\ mass} \tag{2}$$

The Total Dissolved Solids (TDS) were calculated using Equation 3:

$$TDS = Ca^{2+} + Na^{+} + Mg^{2+} + K^{+} \tag{3}$$

The Percentage of Sodium (PS) was calculated using Equation 4 and plotted against TDS to determine the dispersivity of the soils:

$$PS = \frac{Na^{2+}}{TDS} * 100 \tag{4}$$

The liquid limit (W_L), plastic limit (W_P), linear shrinkage (L_S), and specific gravity (SG) of the natural and contaminated soils were determined following the British Standard (1990) using soil fractions passing through a 0.045 mm sieve. The W_L was determined using the Casagrande method, while the W_P was assessed using the thread-rolling test. L_S was measured using a half-cylindrical brass mold of approximately 14 cm in length and 1.25 cm in radius. SG was determined by the pycnometer method.

3. Results and discussion

3.1. Properties of the natural soils

The properties of the natural soils prior to oil contamination are summarized in Table 1. The W_L of the soil samples ranges from 40.2% (L2) to 57% (L4), indicating variability in water-holding capacity. The W_P varies between 25.9% (L2) and 32% (L4), while the plasticity index spans from 14.3% (L2) to 26.1% (L3). These values suggest that the soil samples exhibit moderate to high plasticity, with L2 being the least plastic and L3 the

Table 1. Physical, geochemical and mineralogical properties of the natural soils.

S/N	L1	L2	L3	L4
Liquid limit (%)	51.9	40.2	52.3	57
Plastic limit (%)	28.4	25.9	26.2	32
Plasticity index (%)	23.5	14.3	26.1	25
Specific gravity	2.55	2.53	2.58	2.5
Linear shrinkage (%)	10.6	9.8	10.4	11.1
Quartz (%)	35	30	39	40
Plagioclase (%)	12	8	11	0
K-feldspar (%)	16	25	24	23
Mica (%)	15	12	12	9
Kaolinite (%)	12	15	14	18
Goethite (%)	10	10	0	10
SiO_2 (%)	54.18	54.98	65.75	60.3
TiO_2 (%)	1.65	0.91	0.8	0.74
Al_2O_3 (%)	20.53	20.19	14.99	19.51
Fe_2O_3 (%)	10.28	9.49	7.94	8.05
MgO (%)	1.01	0.32	0.26	0.19
MnO (%)	0.05	0.08	0.16	0.07
CaO (%)	0.93	0.31	0.6	0.21
Na_2O (%)	0.23	0.13	0.38	0.13
K_2O (%)	2.59	4.37	4.85	4.21
P_2O_5 (%)	0.23	0.07	0.08	0.06
LOI (%)	7.84	7.43	4.37	6.71

most. SG values range from 2.50 (L4) to 2.58 (L3), reflecting the mineralogical composition of the soils. LS percentages, which measure the soil's tendency to shrink upon drying, are relatively consistent across samples, with L2 showing the lowest shrinkage (9.8%) and L4 the highest (11.1%).

Quartz is a dominant mineral in all samples, comprising 30% to 40% of the soil composition. The abundance of quartz contributes to the overall strength and durability of the soils. Feldspar minerals, including plagioclase and K-feldspar, are also significant, with their combined concentrations ranging from 28% to 35%. Notably, sample L4 lacks plagioclase but contains 23% K-feldspar, indicating variations in feldspar content among the samples. Mica, a phyllosilicate mineral, is present in all samples, ranging from 9% (L4) to 15% (L1), adding to the soils' plasticity and affecting their engineering properties. Kaolinite, the sole clay mineral identified, is found in concentrations between 12% (L1) and 18% (L4). This suggests that the soils have moderate clay activity, which could influence their plasticity and shrinkage behavior. The presence of goethite in all samples except L3 further contributes to the soil's mineralogical composition, providing additional stability and affecting the soil's color.

In terms of chemical composition, silica (SiO_2), alumina (Al_2O_3), and iron oxide (Fe_2O_3) are the predominant oxides in all samples. SiO_2 content ranges from 54.18% (L1) to 65.75% (L3), with higher silica content correlating with increased quartz percentages. Al_2O_3 concentrations vary between 14.99% (L3) and 20.53% (L1), reflecting the presence of aluminosilicate minerals like feldspars and kaolinite. Fe_2O_3 levels are consistently high, indicating the presence of iron-bearing minerals such as goethite, which is present in all samples except L3.

The Loss on Ignition (LOI), which measures the amount of volatile materials in the soil, is lowest in Sample L3 (4.37%), indicating a relatively lower organic content or fewer volatiles compared to the other samples. This lower LOI value could be related to the

higher quartz content and lower presence of other minerals that contribute to volatilization upon heating.

3.2. Effect of oil contamination on the index properties of the soils

The index properties examined in this study include W_L, W_P, linear shrinkage, and specific gravity. Oil contamination significantly impacted these properties across all soil samples. Notably, there was a substantial increase in the W_L, W_P, plasticity index, and linear shrinkage, while SG decreased (Table 2). These changes suggest that oil contamination affects the soil's physical characteristics, making it more plastic and less dense.

The increase in soil plasticity is evident in the Casagrande plasticity chart (Figure 3), where the contaminated soils plot further away from the high plasticity demarcation line. This finding aligns with previous studies by (Abousnina et al. 2015), which also reported an increase in plasticity due to oil contamination. According to (Carter and Bentley 1991), the plasticity index is

Table 2. Index properties of the natural and crude oil contaminated soils.

		W_L (%)	P_L (%)	PI (%)	SG	L_S (%)
L1	Natural soil	51.9	28.4	23.5	2.55	10.6
	Contaminated soil	65.8	38.7	27.1	2.46	13.5
	Change (%)	26.8	36.3	15.3	−3.5	27.4
L2	Natural soil	40.2	25.9	14.3	2.53	9.8
	Contaminated soil	69.4	39.3	30.1	2.41	13.1
	Change (%)	72.6	51.7	110.5	−4.7	33.7
L3	Natural soil	52.3	26.2	26.1	2.58	10.4
	Contaminated soil	61.5	33.2	28.3	2.43	12.2
	Change (%)	55.8	51.1	60.5	−4.7	31.7
L4	Natural soil	57	32	25	2.5	11.1
	Contaminated soil	72.9	42.3	30.6	2.37	13
	Change (%)	27.9	31.0	19.8	−5.3	15.6

W_L liquid limit; W_P: plastic limit; L_S: linear shrinkage: SG: specific gravity.

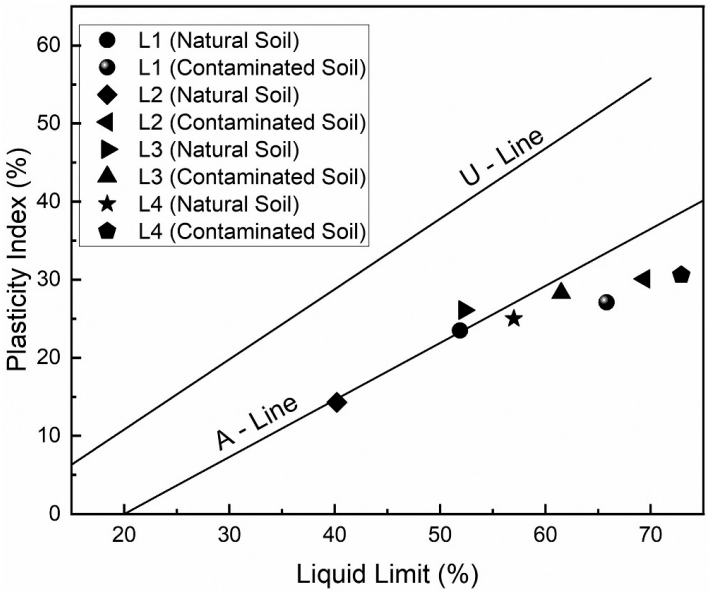


Figure 3. Casagrande chart showing the change in plasticity of the soils due to contamination.

Table 3. Statistical T-test results for the properties of the uncontaminated and contaminated soils.

	Levene's Test for Equality of Variances		t-test for Equality of Means						
								95% Confidence Interval of the Difference	
	F	Sig.	t	df	Sig. (2-tailed)	Mean Difference	Std. Error Difference	Lower	Upper
W_L	0.320	0.592	−3.937	6	0.008	−17.050	4.331	−27.647	−6.453
P_L	0.138	0.723	−4.341	6	0.005	−10.250	2.361	−16.027	−4.473
PI	3.314	0.119	−2.417	6	0.052	−6.800	2.814	−13.685	0.085
SG	0.035	0.858	4.844	6	0.003	0.123	0.025	0.061	0.184
LS	0.000	1.000	−6.467	6	0.001	−2.475	0.383	−3.411	−1.539

a measure of a soil's sensitivity to moisture changes. The observed increase in PI indicates that the oil-contaminated soils have a higher capacity to absorb water, making them less stable under load until a significant change in moisture content occurs.

Sample L2 exhibited the most significant increase in Atterberg limits and linear shrinkage, which is particularly noteworthy given that in its natural, uncontaminated state, L2 had the lowest Atterberg limits, linear shrinkage, and quartz content (Table 3). This suggests that L2 is highly sensitive to oil contamination, with its physical properties being more severely altered compared to the other samples.

The strong correlation between the plasticity index and the remolded shear strength and compressibility of soils, as noted by (Carter and P 1991), implies that the increase in PI observed here corresponds to a reduction in soil strength and an increase in compressibility due to oil contamination. Furthermore, the observed increase in L_S indicates that the contaminated soils are more prone to cracking, shrinking, and expanding characteristics that could have significant implications for the structural stability of foundations and other engineering applications involving these soils (Widjaja 2021).

A paired t-test was employed to assess the significance of differences between the geotechnical properties of uncontaminated and contaminated soils. The results of the t-test (Table 3) indicated significant differences in properties such as W_L, P_L, PI, SG, and L_S between the natural (uncontaminated) and contaminated soils ($p < .05$). These findings suggest that contamination has a statistically significant impact on the geotechnical properties of the soil.

In summary, oil contamination has led to a marked increase in the plasticity and shrinkage potential of the soils, while decreasing their specific gravity. These changes suggest that the contaminated soils would be less stable, more compressible, and prone to greater volume changes, making them less suitable for use in construction without remediation.

3.3. Effect of oil contamination on the dispersivity of the soils

Dispersive soils are highly susceptible to erosion due to their high content of exchangeable sodium ions. These soils are particularly concerning because they are prone to breaking down and dispersing in water, leading to erosion and other geotechnical issues (Umesh, Dinesh, and Sivapullaiah 2011). The PS is a key indicator of sodium ion concentration in soil, with values higher than 60% typically signifying dispersive behavior (Fan and Kong 2013).

In the natural, uncontaminated state, the PS of the studied soils ranges from 54% to 61%, with only one sample (L4) reaching 61%. However, upon contamination, the PS increases across all

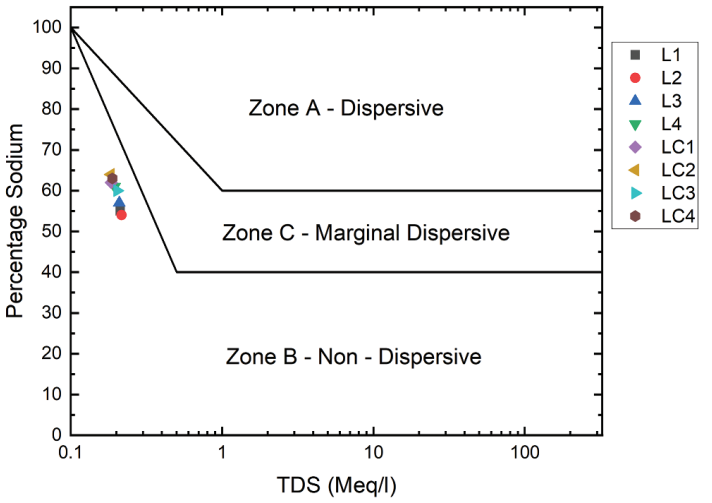


Figure 4. Potential dispersivity chart based on TDS and PS (after (Sherard, Dunnigan, and Decker 1976)).

samples, ranging between 60% and 63%. This increase suggests that oil contamination exacerbates the soils' susceptibility to dispersion. The presence of exchangeable sodium and the amount of total dissolved solids (TDS) in the pore water largely determine a soil's dispersive behavior; higher sodium levels correlate with greater dispersion potential, while lower TDS further increases this susceptibility (Bell and Maud 1994).

To evaluate this relationship, the TDS was plotted against the PS using a criterion established by (Sherard, Dunnigan, and Decker 1976) as cited in (Bell and Walker 2000). Although the soil samples do not fit perfectly into the established demarcation lines, a clear trend is observed: the contaminated samples shift into the region identified as dispersive soils, whereas the natural soils are classified as marginally dispersive (Figure 4). It is important to note that this classification chart was developed for soils from temperate regions, while the studied soils are tropically weathered residual soils. This discrepancy might explain why the samples do not align perfectly with the established classification lines.

Given these findings, there is a need for more research on tropically weathered residual soils, which are common in tropical regions like the study area. Developing a more suitable classification system for these soils will aid in the easy identification of dispersiveness, which is crucial for construction and foundation work in the tropics. Soil dispersivity is closely linked to its erodibility and susceptibility to piping in earth embankments (Gerber and Von 1987). As many earth dams are constructed using locally available residual materials, it is vital to pay close attention to soil dispersivity to prevent dam failures and severe erosion.

Atterberg limits and clay content are critical physical properties influencing soil dispersivity (Fan and Kong 2013). The observed increase in both shrinkage capacity and plasticity in the contaminated soils suggests a possible relationship between increased plasticity and dispersivity (Nagy, Nagy, and Kopecskó 2016, Sherard, Dunnigan, and Decker 1976).

3.4. *Effectiveness of LTTD thermal desorption on the contaminated soils*

The effectiveness of LTTD in remediating contaminated soils was assessed by measuring weight changes before and after the remediation process, while accounting for soil moisture

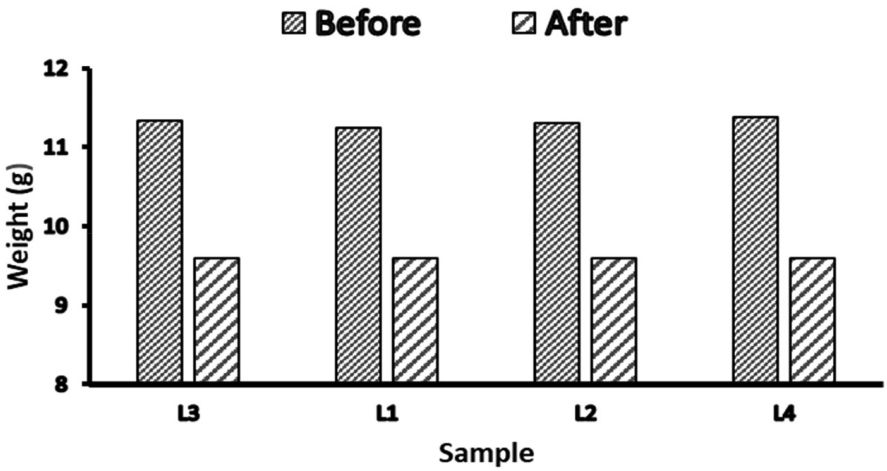


Figure 5. Comparison of contaminated soil weights before and after remediation.

content. A consistent 15% reduction in weight was observed across all samples after oven drying for 30 minutes (Figure 5). This weight loss is primarily attributed to moisture loss during the drying process. To provide a more precise assessment, the removal efficiency was determined based on the initial and final hydrocarbon content of the four predominant hydrocarbons identified through GC-MS: Heptadecane, Pentadecane, 2,6,10,14, Pentacosane, and Nonadecane (Table 4). Post-remediation, the concentration of these hydrocarbons decreased markedly, demonstrating the efficacy of the LTTD process. The average removal efficiency ranged from 30% to 96%, reflecting variable success across different soil samples and indicating that the process effectively targets hydrocarbon volatilization, particularly for heavy hydrocarbons.

Table 4 shows an unexpectedly high removal efficiency for pentacosane, the compound with the highest boiling point (402°C) (Griesbaum et al. 2000). This observation may initially appear counterintuitive, but studies suggest that LTTD can be enhanced by bio-oxidative and soil enzymatic reactions, which effectively lower the desorption temperature needed for hydrocarbons in soils (Liao et al. 2024; Viamajala et al. 2007). These bio-oxidative processes help break down hydrocarbons, facilitating their removal even at temperatures below their typical boiling points. This interaction between thermal and

Table 4. Comparison of hydrocarbon content in contaminated and remediated soils.

SN	Soil Type	Heptadecane	Pentadecane, 2,6,10,14	Pentacosane	Nonadecane
L1	Conc. in unremediated soil (mg/l)	220.04	188.5	87.81	80.54
	Conc. in remediated soil (mg/l)	52.11	45.69	12.55	34.42
	Removal efficiency (%)	76.32	75.76	85.71	57.26
L2	Conc. in unremediated soil (mg/l)	69.22	60.7	18.41	43.83
	Conc. in remediated soil (mg/l)	29.89	26.2	7.46	19.41
	Removal efficiency (%)	57	57	59	56
L3	Conc. in unremediated soil (mg/l)	115.79	101.55	98.37	84.66
	Conc. in remediated soil (mg/l)	5.9	5.16	2.05	3.78
	Removal efficiency (%)	94.9	94.92	97.92	95.54
L4	Conc. in unremediated soil (mg/l)	128.59	125.32	116.07	120.49
	Conc. in remediated soil (mg/l)	97.54	85.55	78.05	83.26
	Removal efficiency (%)	24.15	31.73	32.76	30.9

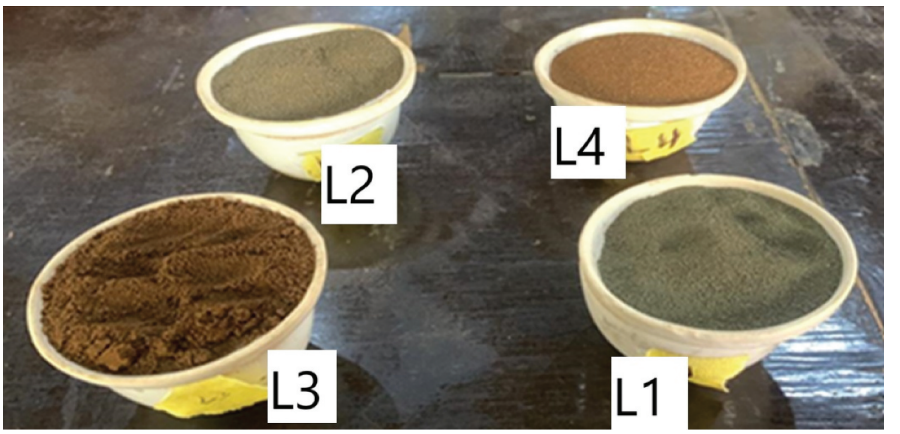


Figure 6. Remediated samples. Note the relatively dark colours of samples L1 and L2 after remediation.

biological mechanisms likely accounts for the high removal efficiency observed for pentacosane, enabling effective desorption within the study's temperature range.

Among the samples, L3 exhibited the highest removal efficiency, while L4 showed the lowest. Notably, L3 also had the lowest Loss on Ignition (LOI) and the highest silica content, suggesting a potential correlation between these properties and the effectiveness of the LTTD process. Conversely, L4, which demonstrated the least removal efficiency, had the lowest feldspar and mica content. However, the differences in mineral content across the samples were not statistically significant enough to definitively link the observed removal efficiencies to the specific mineralogical or chemical characteristics of the soils. The presence of goethite, a mineral that imparts a distinctive color, was noted in samples L1 and L2, both of which contained 10% goethite. This was reflected in their post-remediation coloration (Figure 6). While goethite's role in the remediation process is not fully understood, its presence could potentially influence the thermal desorption outcomes.

This observation underscores the effectiveness of LTTD in reducing hydrocarbon concentrations in contaminated soils. However, the variability in removal efficiency across different soil samples highlights the importance of understanding the influence of soil mineralogy and chemistry on the remediation process. This could help in improving the predictability and optimization of LTTD for various soil types, enabling more efficient and targeted remediation strategies.

3.5. Comparison of Fourier transform infrared (FTIR) spectroscopy for contaminated and remediated soils

The FTIR spectra of the contaminated soils are shown in Figure 7 while the quantitative results of the FTIR of the soils is presented in Table 5. The spectra of the contaminated sample L1C and its remediated counterpart L1R displayed characteristic bands at 3626.5129 and 3699.1345 cm^{-1}, respectively, corresponding to O-H stretching. This indicates the presence of hydroxyl groups in both samples, which are associated with water and possibly alcohols or phenols. Absorption bands at 2924.4959 and 2917.5792 cm^{-1} signify C-H stretching vibrations of the methylene group, indicating the presence of hydrocarbons in the contaminated sample. A significant observation is the presence of a sharp and intense

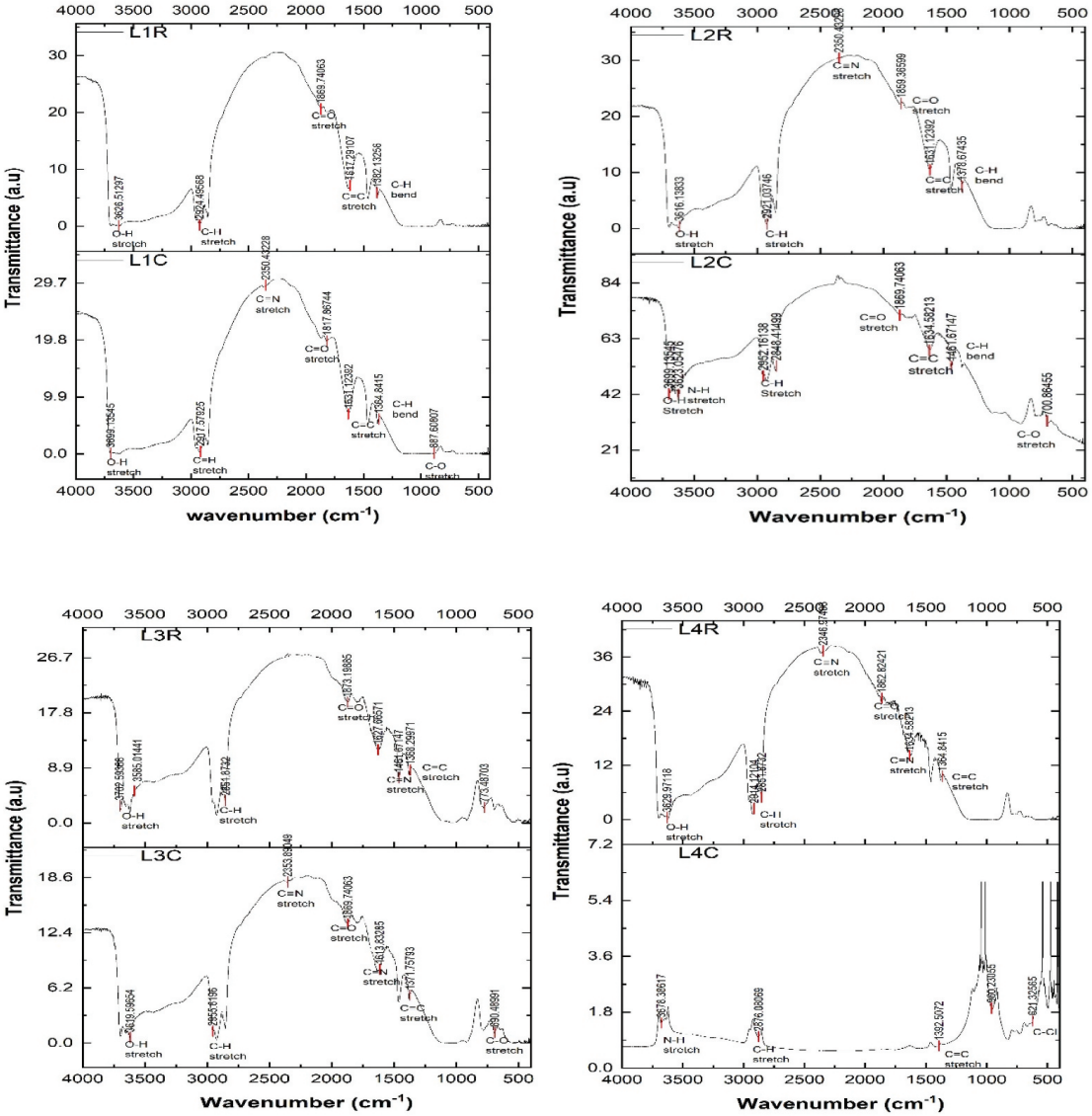


Figure 7. Comparison of FT-IR spectra of selected contaminated and remediated samples (L1, L2, L3, and L4 represent contaminated soil samples; L1R, L2R, L3R, and L4R represent the corresponding remediated samples).

band at 2350.48 cm^{-1}, corresponding to the C≡N stretches of nitrile in sample L1C, which is absent in its remediated counterpart L1R. This suggests that nitrile compounds, which may be part of the crude oil contaminants, were effectively removed by the LTTD process. Additionally, the C-O stretch observed at 887.6080 cm^{-1} in L1C but absent in L1R further indicates the removal of specific organic contaminants through remediation.

The spectra of the contaminated sample L2C and its remediated counterpart L2R displayed similar characteristic bands. The peaks at 700.86 cm^{-1} are the asymmetric stretching vibrations of C – O showing carboxylate groups, confirming the presence of these ligands within the contaminated sample and their absence in the remediated sample. This disappearance of carboxylate groups in L2R supports the effectiveness of the remediation process. In the spectra of remediated sample L3R (Figure 7 and Table 5), the C≡N stretches

Table 5. Quantitative result of FT-IR on the contaminated and remediated samples.

S/N	Peak (Cm^{-1})	Functional Group	Remark
L1C(contaminated)			
1.	3622,00	–OH	Hydroxyl group of alcohol or phenol
2.	2924,29	–CH stretching	CH of sp^3 aliphatic compound
3.	1631,00	C=O stretching	C=O stretching of carbonyl of ester
4.	1460,14	C-H bending	C-H of aliphatic
L1R(remediated)			
1	3623,00	–OH	Hydroxyl group of alcohol or phenol
2.	2923,29	–CH stretching	C-H of aliphatic
3	1629,00	C=O stretching	C=O stretching of carbonyl
4	1459,14	C-H bending	C-H of aliphatic
L2C(contaminated)			
1	3699,36	–OH	Hydroxyl group of alcohol or phenol
2	2926,29	–CH stretching	C=C stretching of aromatic
3	1633,00	C=O stretching	C=O stretching of carbonyl
5	1457,00	C-H bending	C-H of aromatic
L2R(remediated)			
1	3622,00	–OH	Hydroxyl group of alcohol or phenol
2	2924,29	–CH stretching	C-H of aliphatic
3	1632,00	C=O stretching	C=O stretching of carbonyl
4	1458,14	C-H bending	C-H of aliphatic
L3C(contaminated)			
1	3697,36	–OH	Hydroxyl group of alcohol or phenol
2	2923,29	–CH stretching	C=C stretching of aromatic
3	1864,18	C=O stretching	C=O stretching of carbonyl of ester
4	1633,00	C=O stretching	C=O stretching of carbonyl
5	1460, 14	C-H bending	C-H of aromatic
L3R(remediated)			
1	3696,36	–OH	Hydroxyl group of alcohol or phenol
2	2923,29	–CH stretching	C=C stretching of aromatic
3	1870,00	C=O stretching	C=O stretching of carbonyl of ester
4	1628,00	C=O stretching	
5	1459,14	C-H bending	C-H of aromatic
6	1029,00	C-O stretching	C-O of alcohol
L4C(contaminated)			
1	3696,36	–OH	Hydroxyl group of alcohol or phenol
2	2923,29	–CH stretching	C=C stretching of aromatic
3	1633,00	C=O stretching	C=O stretching of carbonyl
4	1462,14	C-H bending	C-H of aliphatic
5	1010,00	C-O stretching	C-O of alcohol
L4R(remediated)			
1	3622,00	–OH	Hydroxyl group of alcohol or phenol
2	2924,29	–CH stretching	C-H of aliphatic
3	1635,00	C=O stretching	C=O stretching of carbonyl
4	1457,00	C-H bending	C-H of aliphatic

bands of nitrile at 2350.48 cm^{-1}, present in the contaminated sample L3C, are absent, demonstrating the removal of nitrile compounds. However, C=N stretches bands of imine appear in both contaminated and remediated samples, suggesting that some nitrogen-containing compounds may persist post-remediation but possibly in altered forms.

The spectra of the contaminated sample L4C displayed characteristic bands at 3629.9711 cm^{-1} due to the stretching vibration of the O – H bonds from surface-absorbed water, which is less intense in the dehydrated form (L4R). The N-H in L4C, identified as a secondary amine, shows a weak band at 3678.3881 cm^{-1}, which may indicate partial transformation during remediation. The C-H stretching vibrations of the methylene group were present in both L4R and L4C, indicating the presence of hydrocarbons in both samples. The presence of an intense band at 2346.97 cm^{-1} (C≡N stretches of nitrile) and

1634.58 cm^{-1} (C=N stretches of imine) in remediated sample L4R, but absent in L4C, suggests the transformation of some organic contaminants rather than their complete removal. The absorbance band at 1862.82 cm^{-1}, indicating the stretching vibration of (C=O) bonds found in COO-, present in L4R but not in L4C, confirms the conversion of certain organic contaminants during the remediation process. The C=C stretches in aromatic rings and the C-Cl stretches observed in the region 621.33 cm^{-1} in L4C but absent in L4R further support the efficacy of the remediation process in reducing specific contaminant groups.

The FT-IR spectra (Figure 7) revealed the presence of C-Cl stretching, nitrogen- and oxygen-containing compounds, and aromatics in the contaminated soils. These results indicate the presence of functional groups that may originate from either the crude oil used or the soil matrix itself. Chlorinated compounds, while not typical in all crude oils, could occur as trace contaminants introduced naturally or through chemical additives during oil processing. Their minimal presence may influence hydrocarbon interactions with the soil particles, affecting adsorption and desorption behaviors. The nitrogen- and oxygen-containing compounds, along with aromatics, are consistent with the composition of heavier fractions of crude oil, which commonly contain heteroatoms. These polar functional groups can increase hydrocarbon polarity, leading to stronger interactions with specific soil minerals. For instance, in soils with lower quartz content, such as L1 and L2, these polar interactions may enhance adsorption. While Table 4 highlights the prominent n-alkanes targeted in the GC-MS analysis, FT-IR provides a broader spectrum of functional groups, including those not explicitly listed in the table. These compounds could influence the efficiency of LTTD. Polar and chlorinated compounds, for example, often require higher energy for volatilization, potentially contributing to the variation in removal efficiencies observed among the samples. This may explain the lower removal rates for L4, which could be attributed to the specific interactions between hydrocarbons and the soil composition.

The FTIR findings show the successful removal and transformation of various organic contaminants from the crude oil-contaminated soils through the LTTD process. The disappearance of nitrile, carboxylate, and other functional groups in the remediated samples indicates the process's effectiveness in reducing the contaminant load, thereby improving soil quality.

3.6. Impact of contamination and remediation on soil mineralogy

X-ray diffraction analysis was conducted to compare the mineralogy of the natural soil samples with those of the remediated contaminated soils, as illustrated in Figure 8. The results reveal no significant changes in mineralogy post-remediation. Similarly, the quantitative analysis presented in Figure 9 confirms that the mineralogical composition of the soils remained largely unaffected by both contamination and the LTTD process. However, the content of some minerals exhibited slight variations due to contamination and the LTTD process (Figure 9). In soils L1, L2, and L3, quartz content increased with contamination and desorption, while in L4, quartz content decreased. For plagioclase feldspar, this mineral was present in the uncontaminated sample of L1 but absent in the remediated sample. In contrast, plagioclase feldspar content increased in L2 and decreased in L3 after contamination and thermal desorption. K-feldspar and mica generally decreased across L1, L2, L3, and

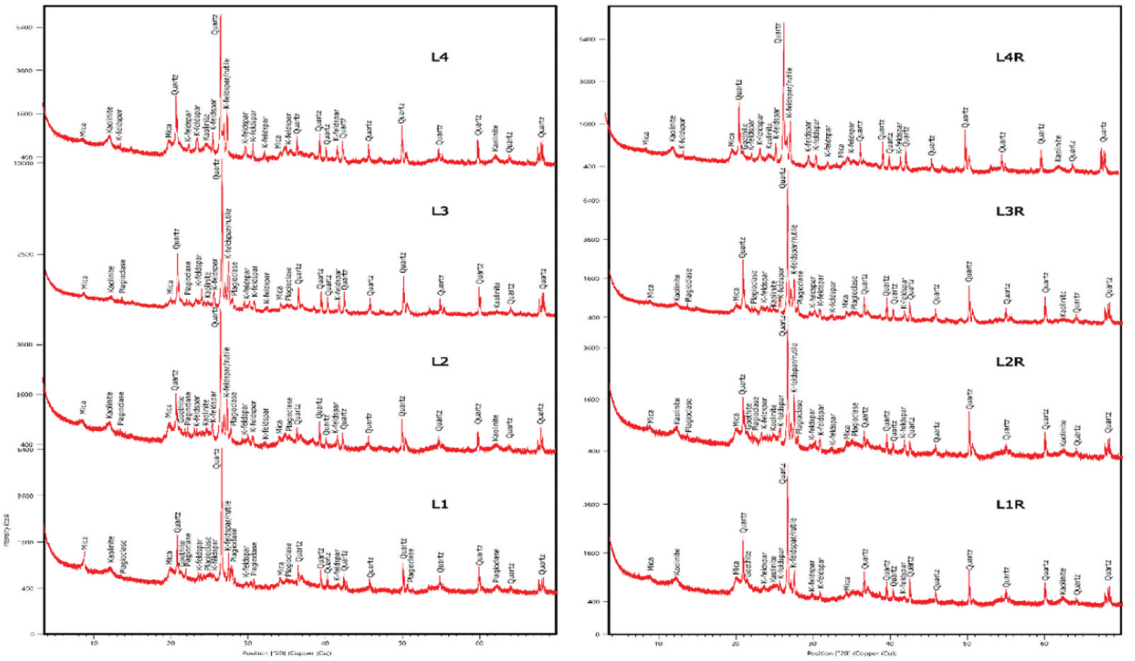


Figure 8. X-Ray diffractograms of the natural and remediated soil samples.

L4 soils due to contamination and thermal desorption, with the exception of L4, where K-feldspar showed a slight increase. Kaolinite content exhibited a minimal increase after contamination but remained unchanged following thermal desorption in L2 and L4. Goethite content increased slightly in L1 and decreased in L2 after contamination and thermal desorption, while it was not detected in L3 or in the uncontaminated sample of L4. Moreover, contamination and the LTTD process did not significantly alter the peak positions of key minerals such as kaolinite, goethite, and quartz. This observation aligns with findings from Afolagboye et al. (2023) and Liu, Liu, and Hu (2015).

The stability of the soil's mineralogical composition despite contamination and remediation can be attributed to the inherent resilience of the minerals present. Quartz, feldspars, mica, and kaolinite, which are predominant in these soils, are chemically stable and resistant to thermal processes at the low temperatures used during LTTD (Afolagboye et al. 2023). These minerals typically require much higher temperatures to undergo any significant chemical or structural changes (Ketterings, Bigham, and Laperche 2000), explaining why their composition remained largely unaffected during the remediation process. Consequently, the effectiveness of LTTD in hydrocarbon removal was achieved without compromising the fundamental mineral structure of the soils.

3.7. Effect of low temperature thermal desorption on microstructure of contaminated soils

The Scanning Electron Micrographs (SEM) of natural soils were compared with those of remediated samples, as shown in Figure 10. The micrographs reveal notable agglomeration of soil particles following remediation, indicating that the LTTD process affected the soil structure. Although no visible traces of crude oil remain in the soil matrix, remnants of

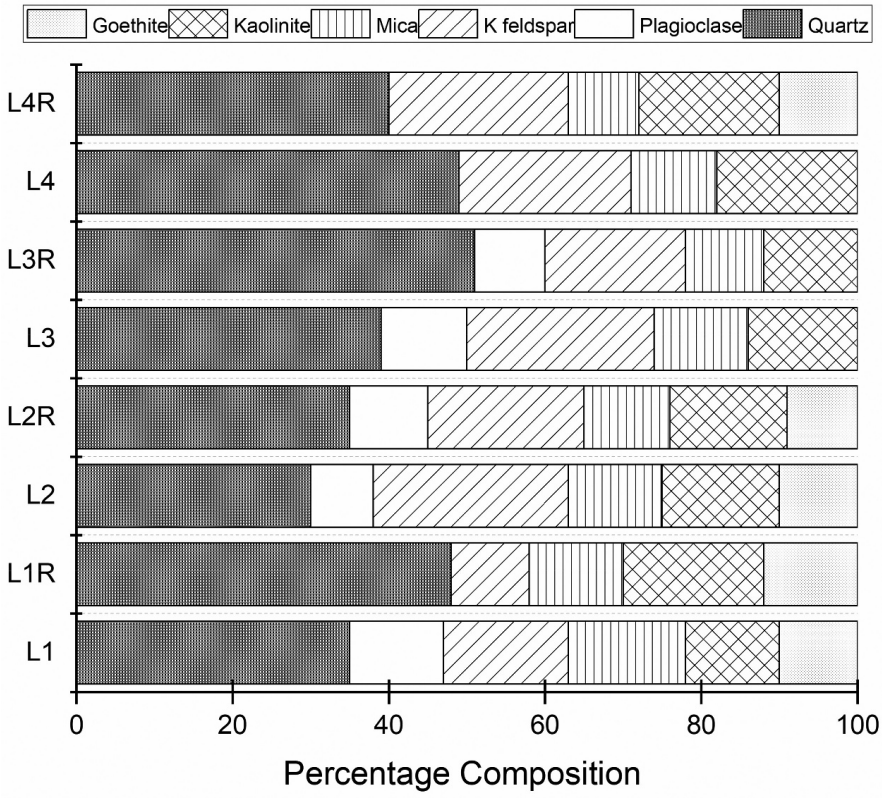


Figure 9. Comparison of quantitative mineralogical composition of natural and remediated soils. l1: l1 contaminated soil; l1r: l1 remediated soil; l2: l2 contaminated soil; l2r: l2 remediated soil; l3: l3 contaminated soil; l3r: l3 remediated soil; l4: l4 contaminated soil; l4r: l4 remediated soil.

adsorbed oil are evident as a coating on the soil particles, even after they were layered with carbon. This oil coating suggests that while LTTD effectively removed most hydrocarbons, some residual oil remains bound to the particles.

Additionally, the SEM images indicate a reduction in porosity, with soil particles appearing more densely packed after remediation. This reduction in porosity likely results from the agglomeration process, where soil particles fuse or cluster together under the influence of heat, reducing the spaces between them. The observation that thermal remediation, even at a relatively low temperature of 110°C, leads to particle agglomeration is consistent with findings reported by (O'Brien et al. 2018). This suggests that the LTTD process not only removes contaminants but also alters the microstructure of the soils, potentially affecting their permeability and other related properties.

4. Conclusion

Soil samples spiked with crude oil from the Nigerian Niger Delta were investigated for changes in their physical and chemical properties, and the effectiveness of LTTD at 110°C was assessed. The study revealed that crude oil contamination significantly increased the plasticity and shrinkage properties of the soils, raising concerns about potential foundation stability issues. Additionally, changes in total dissolved solids (TDS) and PS indicated an increase in soil dispersivity, which could make contaminated soils more susceptible to

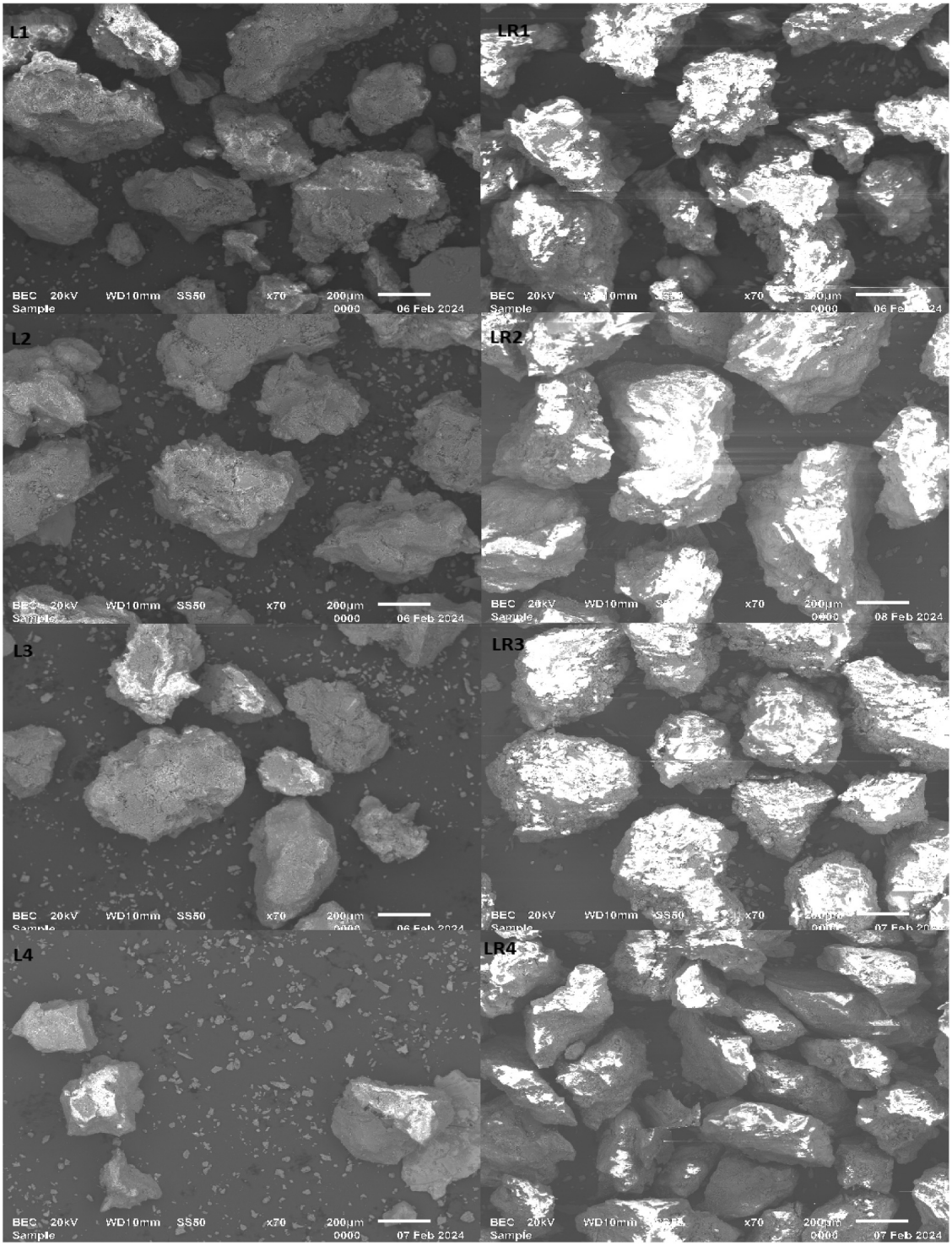


Figure 10. SEM images of natural and remediated soils (L1, L2, L3, and L4 are contaminated soil samples; L1R, L2R, L3R, and L4R are the corresponding remediated samples).

erosion. LTTD at 110°C effectively removed up to 96% of hydrocarbons from the contaminated soils. However, this remediation process also led to a reduction in soil porosity and caused agglomeration of soil particles, as observed through microstructural analysis. This agglomeration may help mitigate the increased dispersivity resulting from oil contamination, potentially reversing some of its negative effects. Importantly, X-ray diffraction analysis showed no significant mineralogical changes in the soils due to either contamination or LTTD remediation, indicating that the fundamental mineral structure of the soils remained largely unaffected. These findings suggest that while LTTD is effective for contaminant removal, its impact on the structure and behavior of residual soils, such as lateritic soils, must be carefully considered, particularly in engineering contexts where soil stability is critical. LTTD at lower temperatures offers promise for addressing crude oil-induced soil degradation, aligning with sustainable environmental management objectives. Future research should focus on understanding the influence of residual soil mineralogy and chemistry on LTTD efficacy and ensuring the structural integrity of treated soils, with the aim of optimizing remediation strategies for various soil types.

Disclosure statement

The authors hereby declare that there is no conflict of interest on the work reported here. All co-authors have seen and agree with the contents of the manuscript and there is no financial interest to report. This paper is an original work conducted by the authors and it is not under review elsewhere.

Author contributions

All authors contributed to the conception and design of the work. Material preparation and laboratory analysis were done by Megan Welman- Purchase, Damilola Tope Ogundele, Olubunmi Oluwadare Owoyemi and Lekan Olatayo Afolagboye. Data analysis and first draft of manuscript was prepared by Olubunmi Oluwadare Owoyemi and Lekan Olatayo Afolagboye. All authors have read and approved the final version of the manuscript.

Data availability statement

They are included in the article

References

Abousnina, R. M., A. Manalo, J. Shiau, and W. Lokuge. 2015. Effects of light crude oil contamination on the physical and mechanical properties of fine sand. *Soil And Sediment Contam An Int J* 24 (8):833–45. doi: 10.1080/15320383.2015.1058338.

Afolagboye, L. O., Z. O. Arije, A. O. Talabi, and O. O. Owoyemi. 2023. Effects of pre-test heating temperature on microstructure, chemical and mineralogy of lateritic soil. *Phys Chem Of The Earth, Parts A/B/C* 132:103504. doi:10.1016/j.pce.2023.103504.

Ahmad, A. A. 2020. Remediation methods of crude oil contaminated soil. *World J Agriculture Soil Sci* 4 (4):1–8. doi: 10.33552/WJASS.2020.04.000595.

Albert, O. N., D. Amaratunga, and R. P. Haigh. 2018. Evaluation of the impacts of oil spill disaster on communities and its influence on restiveness in niger delta, nigeria. *Procedia Eng.* 212:1054–61. doi:10.1016/j.proeng.2018.01.136.

Asghar, H. N., H. M. Rafique, Z. A. Zahir, M. Y. Khan, M. J. Akhtar, M. Naveed, and M. Saleem. 2016. Petroleum hydrocarbons-contaminated soils: remediation approaches. In *Soil science: agricultural and environmental prospectives*, ed. K. R. Hakeem, J. Akhtar, and M. Sabir, 105–29. Springer International Publishing. doi: 10.1007/978-3-319-34451-5_5.

Bashir, I., F. A. Lone, R. A. Bhat, S. A. Mir, Z. A. Dar, and S. A. Dar. 2020. Concerns and threats of contamination on aquatic ecosystems. In *Bioremediation and biotechnology: sustainable approaches to pollution degradation*, ed. K. R. Hakeem, R. A. Bhat, and H. Qadri, 1–26. Springer International Publishing. doi: 10.1007/978-3-030-35691-0_1.

Bell, F. G., and R. R. Maud. 1994. Dispersive soils: A review from a South African perspective. *Q J Eng Geol Hydrogeol* 27 (3):195–210. doi: 10.1144/GSL.QJEGH.1994.027.P3.02.

Bell, F. G., and D. J. H. Walker. 2000. A further examination of the nature of dispersive soils in Natal, South Africa. *Q J Eng Geol Hydrogeol* 33 (3):187–99. doi: 10.1144/qjegh.33.3.187.

Bonatesta, F., C. Emadi, E. R. Price, Y. Wang, J. B. Greer, E. G. Xu, D. Schlenk, M. Grosell, and E. M. Mager. 2022. The developing zebrafish kidney is impaired by *Deepwater Horizon* crude oil early-life stage exposure: A molecular to whole-organism perspective. *Sci Total Environ* 808:151988. doi:10.1016/j.scitotenv.2021.151988.

Buzmakov, S., D. Egorova, and E. Gatina. 2019. Effects of crude oil contamination on soils of the Ural region. *J Soils Sediments* 19 (1):38–48. doi: 10.1007/s11368-018-2025-0

Carter, M. B., and S. P. Bentley. 1991. *Correlations of Soil Properties*. Pentech Press. http://www.amazon.com/Correlations-Soil-Properties-MikeCarter/dp/0727303171/ref=sr_1_1?ie=UTF8&qid=1437878181&sr=81&keywords=Correlations+of+Soil+Properties&pebp=1437878189347&perid=00V4RXV7G18C4685GBB1.

Chuchkalov, S., I. Fadeev, and V. Alekseev. 2020. Effect of synthetic detergents on soil erosion resistance. *KnE Life Sci* 489–96. doi: 10.18502/kls.v5i1.6113.

Falciglia, P. P., M. G. Giustra, and F. G. A. Vagliasindi. 2011. Low-temperature thermal desorption of diesel polluted soil: Influence of temperature and soil texture on contaminant removal kinetics. *J. Hazard. Mater.* 185 (1):392–400. doi:10.1016/j.jhazmat.2010.09.046.

Fan, H., and L. Kong. 2013. Empirical equation for evaluating the dispersivity of cohesive soil. *Can Geotechnical J* 50 (9):989–94. doi: 10.1139/cgj-2012-0332.

Gerber, F. A., and M. H. H. J. Von. 1987. Proposed procedure for identification of dispersive soils by chemical testing. *Civ Engineer In South Africa* 29 (10):397–99. doi: 10.10520/EJC25009.

Ghasemzadeh, H., M. Ostovar, and F. Karimi. 2023. Geotechnical behavior of surfactant-contaminated soils. *Soil Sediment Contam An Int J* 32 (8):1139–56. doi:10.1080/15320383.2023.2171364.

Griesbaum, K., A. Behr, D. Biedenkapp, H.-W. Voges, D. Garbe, C. Paetz, G. Collin, D. Mayer, and H. Höke. 2000. Hydrocarbons. In Ullmann's encyclopedia of industrial chemistry. John Wiley & Sons, Ltd. doi: 10.1002/14356007.a13_227.

Hoseinimighani, H., and J. Szendefy. 2022. A review on mechanisms of thermally induced volume changes in fine soil. *Minerals* 12 (5), Article 5. 572. doi: 10.3390/min12050572.

Kadafa, A. A. 2012. Oil exploration and spillage in the niger delta of nigeria. *Civ Environ Res* 2:38–51.

Kang, C.-U., D.-H. Kim, M. A. Khan, R. Kumar, S.-E. Ji, K.-W. Choi, K.-J. Paeng, S. Park, and B.-H. Jeon. 2020. Pyrolytic remediation of crude oil-contaminated soil. *Sci Total Environ* 713:136498. doi:10.1016/j.scitotenv.2020.136498.

Ketterings, Q. M., J. M. Bigham, and V. Laperche. 2000. Changes in soil mineralogy and texture caused by slash-and-burn fires in Sumatra, Indonesia. *Soil Sci Soc Am J* 64 (3):1108–17. doi: 10.2136/sssaj2000.6431108x.

Kumar, V., P. Kumar, and J. P. Singh. 2020. Environmental Degradation: causes and remediation strategies. *Environmental degradation: causes and remediation strategies*. https://api.semanticscholar.org/CorpusID:216216183.

Liao, J., H. Guo, S. Bordoloi, D. Li, Y. Zhang, J. Ni, H. Yuan, and X. Zhao. 2024. Thermal desorption remediation effects on soil biogeochemical properties and plant performance: Global Meta-analysis. *Biogeotechnics* 100140. doi:10.1016/j.bgtech.2024.100140.

Lim, M. W., E. V. Lau, and P. E. Poh. 2016. A comprehensive guide of remediation technologies for oil contaminated soil—Present works and future directions. *Mar. Pollut. Bull.* 109 (1):14–45. doi:10.1016/j.marpolbul.2016.04.023.

Liu, H., J. Li, M. Zhao, Y. Li, and Y. Chen. 2019. Remediation of oil-based drill cuttings using low-temperature thermal desorption: Performance and kinetics modeling. *Chemosphere* 235:1081–88. doi:10.1016/j.chemosphere.2019.07.047.

Liu, X., X. Liu, and Y. Hu. 2015. Investigation of the thermal behaviour and decomposition kinetics of kaolinite. *Clay Miner.* 50 (2):199–209. doi: 10.1180/claymin.2015.050.2.04.

Magris, R. A., and T. Giarrizzo. 2020. Mysterious oil spill in the Atlantic Ocean threatens marine biodiversity and local people in Brazil. *Mar. Pollut. Bull.* 153:110961. doi:10.1016/j.marpolbul.2020.110961.

McBratney, A., D. J. Field, and A. Koch. 2014. The dimensions of soil security. *Geoderma* 213:203–13. doi:10.1016/j.geoderma.2013.08.013.

Merino, J., and V. Bucalá. 2007. Effect of temperature on the release of hexadecane from soil by thermal treatment. *J. Hazard. Mater.* 143 (1):455–61. doi: 10.1016/j.jhazmat.2006.09.050.

Nagy, G., L. Nagy, and K. Kopecskó. 2016. Examination of the Physico-chemical Composition of Dispersive Soils. *Periodica Polytech Civ Eng* 60 (2), Article 2. 269–79. doi: 10.3311/PPci.8896.

Nasir, M. A., N. P. Canh, and T. N. Lan Le. 2021. Environmental degradation & role of financialisation, economic development, industrialisation and trade liberalisation. *J. Environ. Manag.* 277:111471. doi:10.1016/j.jenvman.2020.111471.

Ndimele, P. E., A. O. Saba, D. O. Ojo, C. C. Ndimele, M. A. Anetekhai, and E. S. Erondu. 2018. Chapter 24—remediation of crude oil spillage. In *The political ecology of oil and gas activities in the Nigerian aquatic ecosystem*, ed. P. E. Ndimele, 369–84. Academic Press. doi: 10.1016/B978-0-12-809399-3.00024-0.

O'Brien, P. L., T. M. DeSutter, F. X. M. Casey, E. Khan, and A. F. Wick. 2018. Thermal remediation alters soil properties – a review. *J. Environ. Manag.* 206:826–35. doi: 10.1016/j.jenvman.2017.11.052.

Ostovar, M., R. Ghiassi, M. J. Mehdizadeh, and N. Shariatmadari. 2021. Effects of crude oil on geotechnical specification of sandy soils. *Soil Sediment Contam An Int J* 30 (1):58–73. doi:10.1080/15320383.2020.1792410.

Portelinha, F. H. M., N. De Souza Correia, I. Santos Mendes, and J. W. B. D. Silva. 2021. Geotechnical properties and microstructure of a diesel contaminated lateritic soil treated with lime. *Soil Sediment Contam An Int J* 30 (7):838–61. doi: 10.1080/15320383.2021.1893648.

Rodrigo-Comino, J., M. López-Vicente, V. Kumar, A. Rodríguez-Seijo, O. Valkó, C. Rojas, H. R. Pourghasemi, L. Salvati, N. Bakr, E. Vaudour, et al. 2020. Soil science challenges in a new era: a transdisciplinary overview of relevant topics. *Air, Soil Water Res* 13:1178622120977491. doi: 10.1177/1178622120977491.

Savaş, H. 2016. Consolidation and swell characteristics of dispersive soils stabilized with lime and natural zeolite. *Sci Eng Composite Mater* 23 (6):589–98. doi:10.1515/secm-2014-0202.

Sherard, J. L., L. P. Dunnigan, and R. S. Decker. 1976. Identification and nature of dispersive soils. *J Geotechnical Eng Div* 102 (4):287–301. doi: 10.1061/AJGEB6.0000256.

Ukhurebor, K. E., H. Athar, C. O. Adetunji, U. O. Aigbe, R. B. Onyancha, and O. Abifarin. 2021. Environmental implications of petroleum spillages in the niger delta region of Nigeria: a review. *J. Environ. Manag.* 293:112872. doi:10.1016/j.jenvman.2021.112872.

Umesh, T. S., S. V. Dinesh, and P. V. Sivapullaiah. 2011. Characterization of dispersive soils. *Mater Sci And Appl* 2 (6), Article 6. 629–33. doi: 10.4236/msa.2011.26085.

Vakili, A. H., J. Ghasemi, M. R. Bin Selamat, M. Salimi, and M. S. Farhadi. 2018. Internal erosional behaviour of dispersive clay stabilized with lignosulfonate and reinforced with polypropylene fiber. *Construct Building Mater* 193:405–15. doi:10.1016/j.conbuildmat.2018.10.213.

Vakili, A. H., M. R. B. Selamat, P. Mohajeri, and H. Moayedi. 2018. A critical review on filter design criteria for dispersive base soils. *Geotechnical Geological Eng* 36 (4):1933–51. doi: 10.1007/s10706-018-0453-7.

Viamajala, S., B. M. Peyton, L. A. Richards, and J. N. Petersen. 2007. Solubilization, solution equilibria, and biodegradation of PAH's under thermophilic conditions. *Chemosphere* 66 (6):1094–106. doi:10.1016/j.chemosphere.2006.06.059.

Wei, Z., Q. Van Le, W. Peng, Y. Yang, H. Yang, H. Gu, S. S. Lam, and C. Sonne. 2021. A review on phytoremediation of contaminants in air, water and soil. *J. Hazard. Mater.* 403:123658. doi:10.1016/j.jhazmat.2020.123658.

Widjaja, B. 2021. Correlation between linear shrinkage value, soil parameters, and soil desiccation cracking pattern. *Prosiding Seminar Nasional Riset Dan Teknologi Terapan (Ritektra)* 12: B5–5.

Wizor, C. H., and E. Wali. 2020. Crude oil theft in the niger delta: the oil companies and host communities conundrum. *Int J Res And Sci Innov* 7 (1):22–32.

Yeeles, A., and A. Akporiaye. 2016. Risk and resilience in the Nigerian oil sector: The economic effects of pipeline sabotage and theft. *Energy Policy* 88:187–96. doi:10.1016/j.enpol.2015.10.018.

Yuan, X., X. Wang, H. Chen, Z. Shi, B. Shi, C. Niu, and T. Ma. 2021. A study on the durability of dispersive soils improved by alum in western Jilin province of China. *Geofluids* 2021 (1):1–10. doi:10.1155/2021/3795958.

Zhao, C., Y. Dong, Y. Feng, Y. Li, and Y. Dong. 2019. Thermal desorption for remediation of contaminated soil: A review. *Chemosphere* 221:841–55. doi:10.1016/j.chemosphere.2019.01.079.